Asian Journal of Chemistry; Vol. 25, No. 13 (2013), 7118-7124

ASIAN JOURNAL OF CHEMISTRY

http://dx.doi.org/10.14233/ajchem.2013.14458

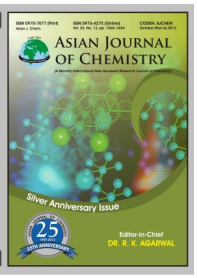

Photophysical and Photochemical Properties of Nanosized Cobalt-Doped TiO_2 Photocatalyst

PALLABI GOSWAMI, RAJIB KUMAR DEBNATH and JATINDRA NATH GANGULI*

Department of Chemistry, Gauhati University, Gauhati-781 014, India

*Corresponding author: Fax: +91 361 2700311; E-mail: jatin_ganguli_gu@yahoo.co.in

(*Received*: 20 August 2012; *Accepted*: 14 June 2013) AJC-13654

Cobalt-doped TiO_2 nanoparticles were prepared by the sol-gel and hydrothermal synthesis methods by using a stable precursor potassium titanium oxalate as Ti source and $Co(NO_3)_2 \cdot 6H_2O$ was used for doping titania. Physicochemical properties of the samples were characterized by XRD, FTIR, RAMAN spectroscopy, DRS, EPR, *etc*. EDX confirmed the presence of cobalt. DRS and TEM revealed that doping has taken place. The calcined materials contained cobalt in (II) state and were found to be room temperature ferromagnetic. The photocatalytic activity of the samples was evaluated by photodecomposition of the dye sunset yellow.

Key Words: Titania, Photocatalysis, Co-doped titania, Sunset yellow dye.

INTRODUCTION

In 2001, Matsumoto and his coworkers[1] discovered room temperature ferromagnetism (RTF) in Co-doped TiO_2 films. That marked the beginning of intense studies on the physical properties of dilute magnetic semiconductors (DMS) for potential applications in optoelectronics, magnetoelectronics, spintronics and microwave devices. It had been a major challenge to induce room temperature ferromagnetism in semiconducting oxides like TiO_2. A number of studies have reported on high temperature ferromagnetism in oxide semiconductors such as TiO_2, ZnO and SnO_2 with TM doping (TM = Co, Ni, Cr, Mn, V and Fe)[2-9]. It has been found that the magnetic properties of cobalt doped titania heavily depend upon the methods and the conditions of sample preparation[10-12]. There is a debate regarding the origin of room temperature ferromagnetism. There are number of reports which showed that room temperature ferromagnetism is intrinsic in nature, others claimed that it might be extrinsic, that is due to the existence of isolated metallic clusters of the doping element. If the samples are prepared at high vacuum or in reducing atmosphere there is a chance that in these cases the observed room temperature ferromagnetism might be arising from metallic cobalt.

Environmental concerns as well as the increasing significance of "green chemistry" synthetic strategies require utilization of new non-toxic precursors compatible with neutral water as a processing solvent. To achieve this object for transition-metal ions in their highest oxidation state such as titanium, niobium and tantalum was especially difficult due to the high susceptibility of these cations to hydrolysis. Substances which were most commonly used as precursor for Ti are titanium tetrachloride, titanium isopropoxide, titanium sulphate, titanium tetrabutoxide, *etc*. But unfortunately, most of the precursors of Ti were found to have some limitations. We have used a water soluble precursor for Ti namely potassium titanyl oxalate which is extremely stable, non-corrosive, not eco-toxic. It is not hazardous according to Directive 67/548/EC. Hazardous decomposition products are only titanium/titanium oxides. With the precursor potassium titanium oxalate both the control of the nanostructure and increase in spectral sensitivity can be achieved. Potassium titanium oxalate dihydrate is soluble in water. The aqueous solution produces a precipitate when treated with ammonia. The novelty of the precursor and the reported process can be summarized as follows- (i) Water is used as a processing solvent which is less costly, environment friendly and can be regarded as a green solvent. (ii) A "gel"-like matter rather than a simple precipitate is formed. (iii) A chelate-type ligand is used as a stabilizer for the constituent metal ions. (iv) The precursor material, obtained after a thermal decomposition of the "gel"-like matter, is found to be amorphous from XRD analysis, ensuring in most cases the compositional homogeneity of the target oxide material.

In this paper we report the preparation of cobalt doped titania from a novel precursor potassium titanyl oxalate. The photocalytic activity of as synthesized and calcined cobalt doped titania was studied by photodegradation of sunset yellow dye in aqueous media. The activities of synthesized samples were compared with undoped as well as commercial titania. The correlation of the catalytic performance to the structural properties and the promoting effect of the Co-modifications were discussed briefly based on systematic characterizations.

EXPERIMENTAL

Photocatalyst preparation: Preparation of Co-doped TiO_2 from cobalt nitrate hexahydrate and potassium titanyl oxalate [$K_2TiO(C_2O_4)_2 \cdot 2H_2O$]: $K_2TiO(C_2O_4)_2 \cdot 2H_2O$ was dissolved in 125 mL distilled water and hydrolyzed by slow addition of NH_4OH solution under constant stirring at room temperature, in a Teflon beaker, until the reaction mixture had attained a pH of 7.5. The precipitate was further dispersed in 250 mL of hot distilled water and peptized by the addition of 10 % HNO_3 solution. Required amount of $Co(NO_3)_2 \cdot 6H_2O$ was added to the solution, which immediately oxidized to Co(III) ions. The solution was then added into surfactant triblock copolymer poly(ethylene glycol)-block -poly(propylene glycol) -block poly(ethylene glycol) $EO_{20}PO_{20}EO_{20}$ solution under stirring. The molar ratio of $K_2TiO(C_2O_4)_2 \cdot 2H_2O$: $Co(NO_3)_2$: surfactant P123:H_2O is 0.9:0.1:0.12:100. After stirring the mixture for 0.5 h, the resulting mixture was aged at room temperature for 12 h and then transferred into a Teflon lined stainless steel autoclave at 373 K for hydrothermal treatment. After 72 h, the resulting mixture was cooled to room temperature, separated by centrifugation, washed with water and ethanol and then dried at 393 K overnight. The organic materials were removed by stirring the titania powders with a water and ethanol solution (molar ratio 1:1) of 0.4 g NaCl at 313 K for 5 h. The resultant solids were washed with water and ethanol and then dried at 393 K overnight. The as-synthesized sample was divided into two parts. One part was calcined in air at 873 K for 6 h with a heating rate of 2 degree/min and the other part is labelled as-synthesized sample. For the purpose of comparison, undoped TiO_2 was prepared by the same method without the use of cobalt nitrate hexahydrate.

Photocatalytic reactions: Sunset yellow, an anionic dye, was selected as the target compound for the photo activity of cobalt doped titania under UV light. An immersion well photochemical reactor (HEBER) made of Pyrex glass was used in this study. Aqueous dispersion of the catalyst was prepared by addition of a given weight (0.2 g) of catalyst to *ca.* 50 mL of aqueous solution of the dye (10^{-5} M) and sonicated in a sonicator for 5 min. The dispersion is then put in to the Pyrex vessel of the photoreactor along with an additional amount of dye solution (10^{-5} M) just enough to fill the vessel. Prior to the illumination, the solutions were purged with air for 15 min to ensure the equilibrium among the catalysts, sunset yellow and oxygen. The dispersions were kept under constant air bubbling with the help of air pump during irradiation. The zero time reading was obtained from blank solution kept in the dark but otherwise treated similarly to the irradiated solution. Irradiations were carried out using a 25 W, 254 nm medium pressure mercury lamp. IR radiation and short wavelength UV radiation were eliminated by a water circulating Pyrex glass jacket. Samples (10 mL) were collected before and at regular intervals during the irradiation for analysis. The degradation of sunset yellow was monitored by measuring the absorbance on a Shimadzu spectrophotometer at 482 nm. Photocatalytic degradation of sunset yellow is a pseudo-first order reaction and its kinetics according to Langmuir-Hinshelwood kinetic model can be expressed as follows: $\ln (C_0/C_t) = kt$, where C_0 and C_t are the initial concentration and the reaction concentration of the dye after time t, respectively.

RESULTS AND DISCUSSION

The XRD patterns of the as synthesized and calcined catalysts are shown in Fig. 1 and compared with the XRD pattern of pure anatase phase (JCPDS No. 84-1286) and pure brookite phase (JCPDS No-29-1360).

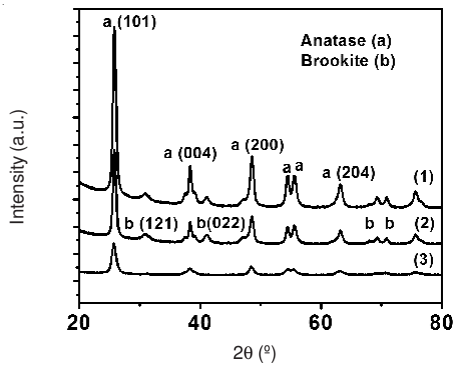

Fig. 1. XRD of calcined Co-doped (1), as synthesized Co-doped (2) and calcined undoped titania (3)

Potassium titanyl oxalate crystal structures as had been reported were solved by analyzing single-crystal X-ray diffraction data[13]. The structure contains tetranuclear anions of chemical composition $[TiO(OX)_2]_4^{8-}$, which form eight-membered rings of four Ti and four O atoms (μ-oxo bridging groups). Each Ti atom is coordinated by two oxalate ions, each forming a five-membered chelate ring. As a result, each Ti atom has a distorted octahedral environment. In the as synthesized cobalt doped nanomaterials cobalt(III) ions may be in octahedral environment replacing Ti(IV) ions in titania matrix. The XRD of cobalt doped titania contained anatase and brookite phases of titania while the undoped titania contained only anatase phase. It has been reported that the XRD peaks at 2θ values of 36.8 and 60º can be attributed to different crystal planes of cobalt oxides and the peaks corresponding to cobalt metal should appear at 2θ values of 43.8 and 51.5º[14]. Absence of these peaks indicates that probably some Co(III) ions replaced Ti(IV) ions in the crystal framework of TiO_2. Average crystal sizes calculated from the broadening of the (101) peak of anatase phase were *ca.* 8.9 nm for as synthesized cobalt doped titania, while for undoped calcined TiO_2, it is *ca.* 14.5 nm and for calcined cobalt doped titania it was 13.1 nm. The average crystal sizes increased after calcinations because of the growth of the quantum sized grains[15]. It was reported that polymorphous transformation occurs at a wide range of temperatures 673-1373 K, though normally it takes place at *ca.* 1073-1123 K. XRD of the products reveals that no such transforamation to rutile phase took place when calcined upto 873 K.

The surface morphology of as synthesized cobalt doped photocatalyst was studied by scanning electron microscopy and the micrograph is presented in Fig. 2. SEM image showed that as synthesized samples consisted of uniform spherical structure. EDX (Fig. 3) analysis of Co-doped titania samples showed the presence of Co in the mesostructure.

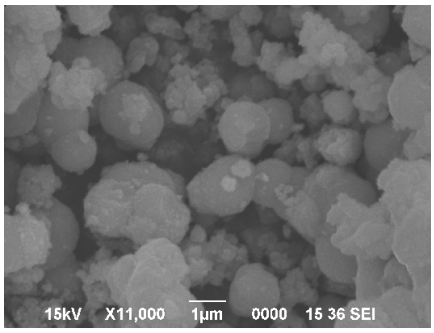

Fig. 2. SEM of as synthesized cobalt doped titania

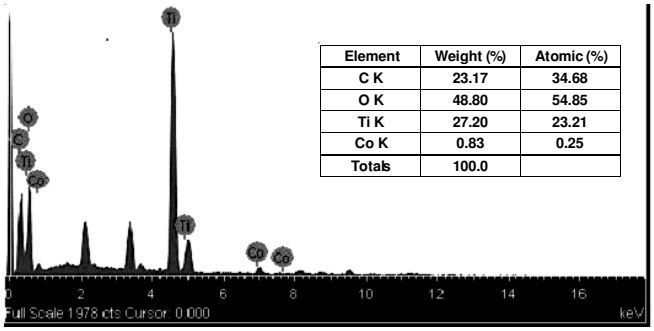

Element	Weight (%)	Atomic (%)
C K	23.17	34.68
O K	48.80	54.85
Ti K	27.20	23.21
Co K	0.83	0.25
Totals	100.0	

Fig. 3. EDX of calcined cobalt doped titania

Figs. 4 and 5 display the HRTEM images of the calcined cobalt doped titania sample. As shown in Fig. 4, cobalt doped titania exhibits uniform spherical particles. It seems from Fig. 5 that well-crystallized anatase of *ca.* 10 nm in size is dispersed in an amorphous Co-containing titania nanoparticles and the figure clearly displayed well-resolved crystal lattice. Crystal boundaries of well crystallized anatase were clearly evident in high magnification TEM image.

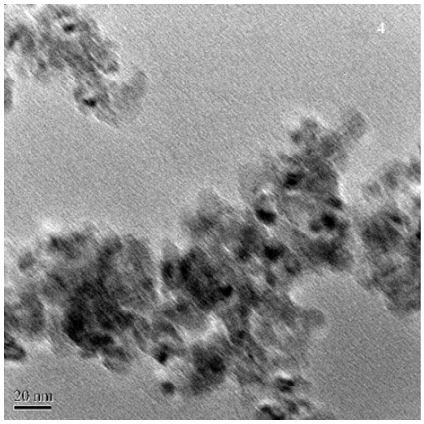

Fig. 4. TEM of calcined cobalt doped titania

The thermal behaviour of as synthesized cobalt doped sample was investigated with TG at temperatures ranging from room temperature to 973K (Fig. 6). The first weight loss at 373-623 K was the dehydration and loss of residual organic materials from the surfaces of the powdered materials. As thermal treatment increases, the remaining water, strongly bonded inside the pores of the particles, can be eliminated thus giving the second weight loss effect at 423 K for P1. In fact, according to findings by Bickley *et al.*[16] the loss of adsorbed molecular water in the range 373-573 K appears to be related to the development of porosity.

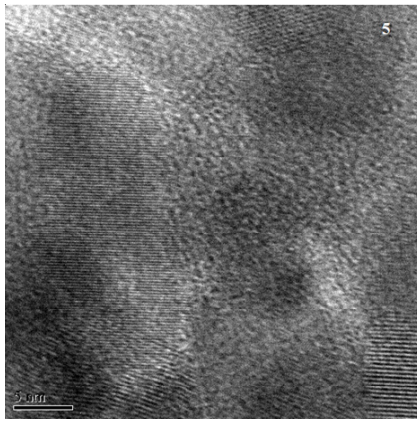

Fig. 5. HRTEM of calcined cobalt doped titania

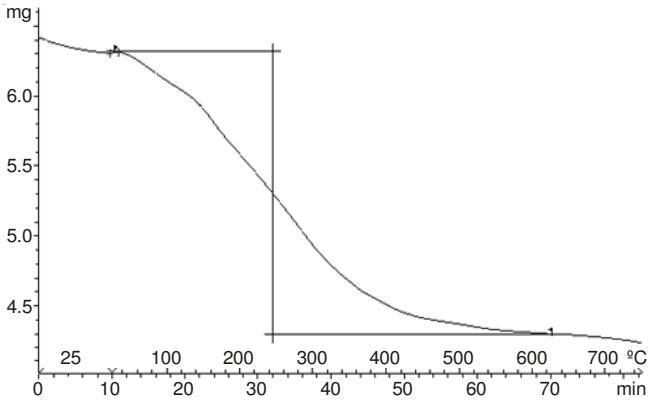

Fig. 6. Thermogravimetric analysis of cobalt doped titania

We have used UV-visible/DRS to study the state of Co in the prepared catalyst. In order to estimate the band energy gap of oxides, we have used the Kubelka-Munk function[17]. The position of the absorption edge can then be determined by extrapolating the linear part of the rising curve to zero. The diffuse reflectance UV-visible spectra of the as synthesized cobalt doped titania, calcined cobalt doped and undoped titania samples are reported in Figs. 7-10. All the samples have in common an intense UV absorption band with a maximum in the range 220-320 nm due to charge transfer from oxygen to titanium(IV)[18-20]. The position of this band is affected by the coordination geometry around the titanium atom and by the presence of adsorbents. More precisely, the bands in the region 210-240 nm are attributed to charge transfer from oxygen to tetrahedral Ti(IV)[21], whereas the bands at higher wavelength ($\lambda > 240$ nm) are due to octahedral Ti(IV) sites[22,23]. The as synthesized cobalt doped titania (Fig. 7) had intense UV absorption band at higher wavelength ($\lambda > 240$ nm) with most of the Ti(IV) ions in the octahedral environment. The calcined cobalt doped titania had mostly Ti(IV) in tetrahedral state as was evidenced from UV peak below 240 nm (Fig. 10)[24-31]. It was anticipated that large differences in optical properties would be required in order to cause changes in photocatalytic behaviour. As expected pure TiO_2 crystals did not show any abrupt variation in the 400 nm range (Fig. 4C.10). The doped samples had comparatively distinct maxima and sharp bands (intense absorption) in the same region. The optical absorption edge (visible region) of the crystals shifted slightly to higher wavelength in doped samples. For undoped titania T

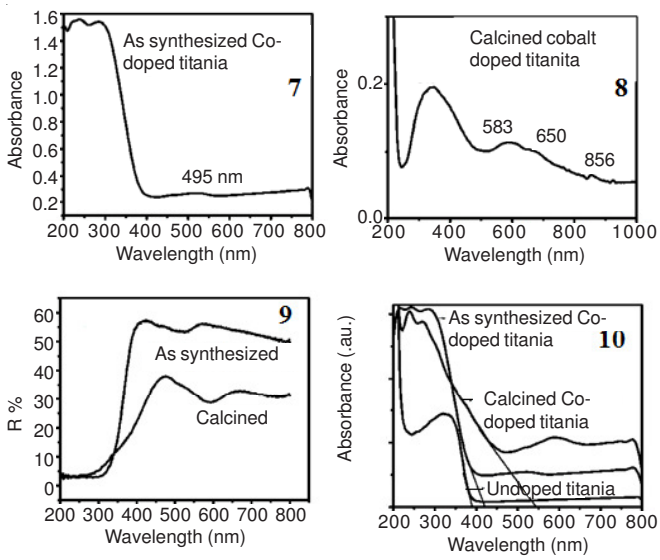

Fig. 7-10. Diffuse reflectance spectra of synthesized samples

the band gap value is *ca.* 3.12 eV which is the recognized band gap of anatase titania. The UV-visible diffuse reflectance measurements showed that doping Co to titania produces a pronounced red shift in the onset of the optical absorption edge of TiO_2 samples in the visible region (Fig. 10). In addition to the charge-transfer bands due to Ti, appearing in the UV region, the visible spectra of these catalysts exhibit bands in the 500-750 nm regions, which are associated with Co species[32,33]. In the case of as synthesized samples, cobalt was in octahedral environment (light pink colour) and was in (III) oxidation state with a d^6 electronic configuration. Only one weak *d-d* transition is observed at *ca.* 495 nm (Fig. 7) which is the $^1T_{1g} \leftarrow {}^1A_{1g}$ transition of cobalt(III) ion.

In the calcined cobalt doped titania three transitions were obtained (Fig. 8) at 587, 627 and 856 nm indicating $^4A_2 \leftarrow {}^4T_1$ and $^4T_1(P) \leftarrow {}^4T_1(F)$ transitions of cobalt(II)[34]. These reflectance spectra obtained for the calcined samples indicates that tetrahedral Co(II) was present in all calcined cobalt doped titania (dark bluish green colour). The band gap values calculated were *ca.* 3.12 eV for undoped titania, *ca.* 2.95 eV for as synthesized cobalt doped titania and for the dark bluish green calcined cobalt doped sample sample was *ca.* 2.29 eV.

Magnetic properties of the synthesized nanoparticles were measured at 300 K and the results are presented in Fig. 11. It is found from Fig. 11 that the calcined Co-doped titanate nanoparticles exhibit an evident hysteresis loops at 300 K, indicating ferromagnetic properties although the cobalt concentration in the calcined samples were very low. Calcined cobalt doped titania with cobalt(II) in tetrahedral state is ferromagnetic at room temperature whereas the as synthesized cobalt doped titania with cobalt in (III) state were diamagnetic in nature as was confirmed from magnetic studies. As no metallic Co and other ferromagnetic phases were detected by the various characterization techniques employed in this work, it is thus plausible to conclude that the ferromagnetism is intrinsic in the samples. It was reported that oxygen vacancies near Co(II) sites in Co-doped TiO_2 had an important contribution to the ferromagnetism[35]. Coey *et al.*[36] proposed that oxygen vacancies induced the ferromagnetic coupling through

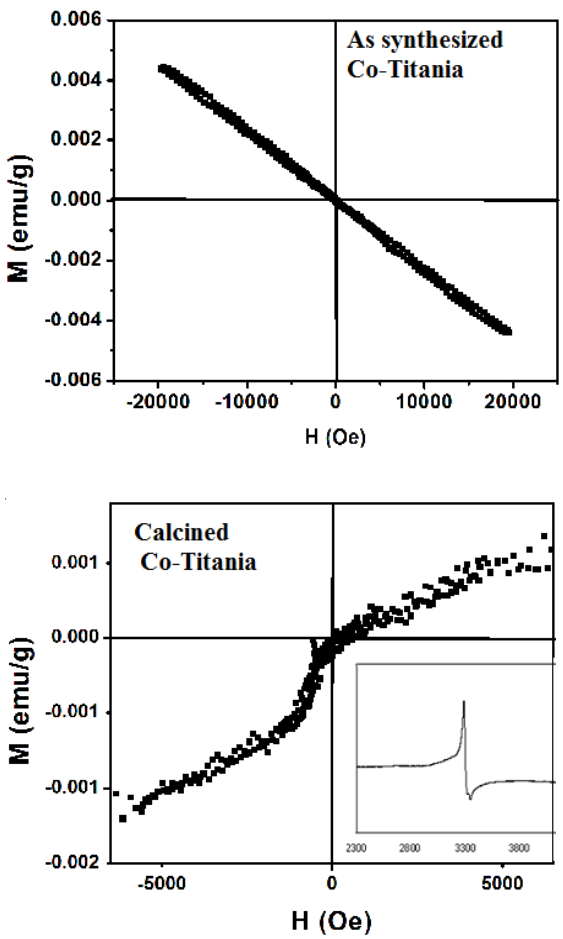

Fig. 11. Magnetic behaviour of as synthesized and calcined cobalt doped titania

a F-center exchange mechanism. Several features like band gap narrowing, shifting and broadening of some of the Raman modes strongly support the incorporation of Co into the TiO_2 lattice. Therefore, ferromagnetism is expected to arise from the intrinsic exchange interaction of magnetic moments mediated by defects in doped nanoparticles.

To further confirm the existence of oxygen vacancies, EPR spectra of the calcined Co-doped titania as inserted in Fig. 11 of calcined cobalt doped titania. It is shown that calcined sample had the sharp symmetric EPR peak. The EPR signal with g = 2.00 was reported and referred to as a single-electron trapped oxygen vacancy of TiO_2[37]. Absence of the asymmetric EPR signal with g = 1.97-1.98 indicates absence of surface defects[37]. It implies that bulk oxygen vacancies rather than surface defects have more responsibility for the appearance of EPR signals in calcined Co-doped titania.

The surface characteristics of synthesized samples, including specific surface area, were determined from nitrogen physisorption (Table-1). The specific surface area of calcined sample showed a decrease when compared with the as synthesized TiO_2 particles, which have a surface area of *ca.* 53 $m^2 g^{-1}$. The implantation of metallic dopants results in a slight increase in the surface area of the cobalt doped samples. Block copolymer used in the synthesis generally results in high surface area but on calcination due to breakage of mesostructure there is decrease in surface area.

TABLE-1
PHYSICAL PROPERTIES OF VARIOUS SYNTHESIZED PHOTOCATALYSTS

Photocatalyst	2θ	hkl	Crystalline size nm	BET surface area (m^2/g)	Band gap (eV)
As synthesized Co-titania	25.7º, 38.26º, 48.40º	(101), (004), (200)	8.9	53	2.95
Calcined Co-Titania	25.75º, 38.35º, 48.55º	(101), (004), (200)	13.1	46	2.29
Undoped titania	25.84º, 38.35º, 48.58º	(101), (004), (200)	14.5	36	3.14
JCPDS 84-1286	25º, 38º, 48º	(101), (004), (200)	–	–	–

In the Raman spectra (Fig. 12) of both pure and cobalt doped calcined samples the dominant modes can be assigned to the Raman active modes of the anatase crystal[38] *ca.* 143 ($E_{g(1)}$), 197 (Eg_2), 399 ($B_{1g(1)}$), 519 (A_{1g}, $B_{1g(2)}$) and 639 cm^{-1} ($E_{g(3)}$). The small difference in the positions of these peaks reflects the difference in the vibrational motions, possibly due to the structural difference because of the possible lattice distortion brought by the Co dopants and/ or oxygen vacancies. The Raman peaks at 398 and 515 cm^{-1} clearly show that the samples are in the anatase phase. Within an experimental accuracy of a few wave numbers, there is no discernable shift of the Raman peaks with Co-doping. However, for the Co-doped samples, the Raman peaks broadened. This may be an indication of limited Co solubility resulting in a disorder of the crystal structure. The widths of these peaks for the TiO_2 increased in the order cobalt doped undoped titania. This suggested that the size of these TiO_2 decreased in the order of undoped titania < cobalt doped, since the width of the peak results from the finite lifetime of the vibrational modes in the small size particles and is inversely proportional to the size of the particle and may be also possibly related to the dopants' influence on the lattice distortion.

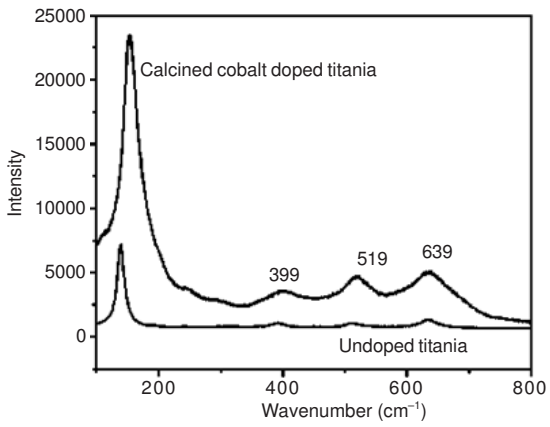

Fig. 12. Raman spectra of calcined cobalt doped and undoped titania

Environmental contamination and serious hazards through misuse of a variety of dyes has attracted global attention. Sunset yellow is a water soluble monoazo dye, has been used since 1929 to impart a reddish-yellow colour to various carbonated beverages, candies, jams, pickles *etc*. Oral provocation tests have indicated that sunset yellow can provoke various symptoms, principally skin complaints and asthmatic reactions, in a small percentage of those exposed. Recently many efforts have been devoted to the solution of increasingly serious environmental problems due to misuse of different dye stuff. Photocatalytic degradation of dyes is most widely accepted process now-a-days. So photodegradation of sunset yellow was used as a probe reaction to test the photocatalytic activity of prepared Co-doped catalysts. The photocatalytic degradation of the dye over the calcined undoped and cobalt doped as well as, as synthesized titania was measured in identical conditions for comparison. The photocatalytic activity of all catalysts was evaluated by measuring the absorbance (A_t) of sunset yellow UV-visible spectrum at 482 nm during every 10 min interval. With the assumption that Beer's law was obeyed, the graph of A_t/A_0 against t (where A_0 is the intensity of dye peak at 482 nm after stirring in the dark for 15 min) is equivalent to the graph of C_t/C_0 against t and the latter was plotted. Fig. 13 showed the relationship between the degradation time and the concentration of sunset yellow during the progress of photocatalytic degradation. Fig. 13 showed that the concentration of dye decreased almost linearly and, finally, the dye solution was almost 60 % decomposed. After stirring in the dark for 15 min, the concentrations of sunset yellow in the suspension with catalyst samples decreased sharply to *ca.* 1 % of the original concentration, which means that some amount of the dye was adsorbed on the TiO_2 powders before the start of photocatalytic degradation, whereas *ca.* 2 % of the dye was adsorbed by as synthesized cobalt doped titania, respectively. The surface of all of the Co-doped TiO_2 powders was coated in orange as a result of the adsorption of dye. With the progress of photocatalytic degradation, the colour of the powders was gradually changed to yellowish and to dirty white, which indicates that the adsorbed dye was degraded.

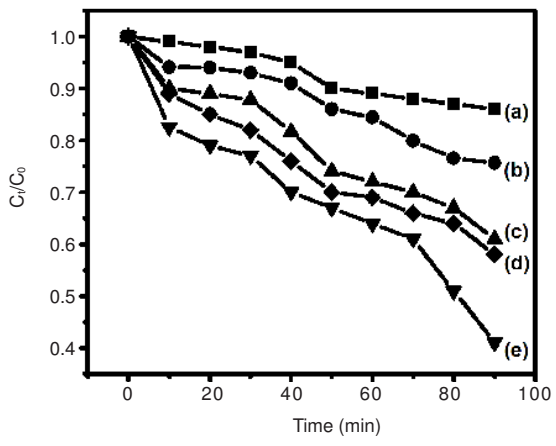

Fig. 13. Photocatalytic decomposition of (a) sunset yellow alone (b) with commercial titania (c) with calcined undoped titania (d) with calcined cobalt doped titania (e) with as synthesized cobalt doped titania

Fig. 14 shows the absorption spectra of the aqueous solution of sunset yellow during the process of photodegradation. From this point of view, the photocatalytic degradation of the solution of sunset yellow has two steps *i.e.*, adsorption and degradation.

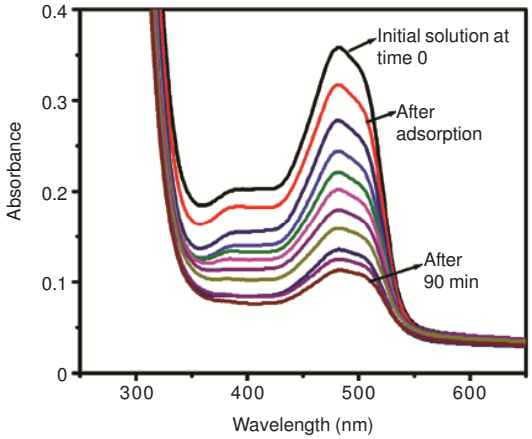

Fig. 14. Decomposition of sunset yellow with calcined cobalt doped titania

At the first stage, the nanocrystalline TiO_2 powders would adsorb the dye molecules due to the higher surface energy, which causes the decrease of the dye concentration before the start of photodegradation then, the dye will be decomposed gradually after being illuminated with UV light irradiation. All of the synthesized Co-doped TiO_2 powders exhibited good photocatalytic activities when decomposing dye solution under UV light irradiation but the as synthesized cobalt doped titania exhibited the maximum photocatalytic activity compared to calcined cobalt doped and undoped titania.

Theoretically, the rate of photocatalysis is determined by several factors one of which is the competitive rate of recombination of photogenerated electron-hole pairs within a semiconductor. The presence of surface state at energies inside the band gap region can either decrease or increase the lifetime of electrons and holes depending upon whether these energy levels function as efficient recombination centers or as surface traps which prolong the life of holes and electrons. Co is well known as good electron conductor. The existence of cobalt on the TiO_2 matrix will help the electron transferring and therefore reduce the possibility of recombination of photogenerated electronhole pairs, which consequently results in higher photocatalytic activity than that of TiO_2 only catalyst. The increase in photoactivity of synthesized Co-doped photocatalysts must be due to interaction between Co(II/III) and Ti(IV) ions in titania. That led to several modifications in physical properties such as band gap, thermal stability, particle size and magnetic properties *etc*. The principle of the semiconductor photocatalytic reaction is straightforward. Upon absorption of photons with energy larger than the band gap of TiO_2, electrons are excited from the valence band to the conduction band, creating electron-hole pairs. These charge carriers migrate to the surface and react with the chemicals adsorbed on the surface to decompose these chemicals. This photodecomposition process usually involves one or more radicals or intermediate species such as $^{\bullet}OH$, O_2^-, H_2O_2 or O_2, which play important roles in the photocatalytic reaction mechanisms. When UV light photon excites an electron from the ground state to the excited state of the undoped titania, then the excited electron is transferred into the conduction band of TiO_2. The conduction band electron is then subsequently transferred to oxygen molecules adsorbed on the catalyst surface directly forming reactive superoxide anions ($O_2 + e_{CB}^- = O_2^{\bullet-}$) that degrade sunset yellow dye on the TiO_2 catalyst surface in a series of reaction events.

When cobalt is present then there is a change in the scenario, as doped cobalt ions act as more efficient electron traps [$Co(III) + e_{CB}^- \rightarrow Co(II)$] than the adsorbed oxygen species. This results in even more efficient migration and separation of conduction band electrons over the as synthesized cobalt doped TiO_2 photocatalyst than undoped TiO_2 producing more mobile holes in the hybridized valence band (O2*p* + Co3*d*)[39] of the cobalt doped TiO_2 photocatalyst at the same photoexcitation event. To rejuvenate the photocatalytic cycle, valence band holes oxidize conduction band electron reduced Co(II) to Co(III) ions [$h_{VB}^+ + Co(II) \rightarrow Co(III)$]. This catalytic cycle of the doped cobalt ions, continues as long as UV light is irradiated over doped TiO_2 catalyst.

$TiO_2 + h\nu \rightarrow h^+ + e^-$ (electron and hole generation)

$Co(III) + e^- \rightarrow Co(II)$

$Co(II) + O_2 \rightarrow Co(III) + O_2^{\bullet-}$

$Co(II) + h^+ \rightarrow Co(III)$

$Co(III) + OH^- \rightarrow Co(II) + {}^{\bullet}OH$

$Dye + {}^{\bullet}OH \rightarrow$ Degraded products

$Dye + O_2^- \rightarrow$ Degraded products

As synthesized cobalt doped titania contained cobalt in (III) oxidation state with octahedral arrangement around the cobalt (light pink coloured), while the calcined sample which was intense green in colour contained cobalt in (II) oxidation state. In Co(III) octahedral arrangement, the metal had a d^6 configuration and most of the ligands are strong enough to cause spin pairing, giving the electronic arrangement $(t_{2g})^6 (e_g)^0$. This arrangement had very large crystal field stabilization energy and was found to be diamagnetic. Cobalt(II) complexes are readily oxidized to Co(III) and this happens because the crystal field stabilization energy of Co(III) with a d^6 configuration is higher than for Co(II) with a d^7 configuration. Thus from the viewpoint of crystal field theory, Co(II) is relatively unstable as compared to Co(III), which had d^6 configuration. Therefore, there was a tendency for the transfer of the trapped charge carriers from Co(II) to the adsorbed O_2 and surface hydroxyl (OH^-), respectively, to regenerate Co(III). These new produced active species (such as OH^- and O_2) will initiate the photocatalytic reactions of decomposition of sunset yellow[40]. Samples taken at 1 h time intervals were analyzed by LC/MS (LCMS-2010 EV liquid chromatography mass spectrometer, Shimadzu) to identify the intermediate compounds as LCMS technique is specifically useful to study the degradation of dye as well as the formation of intermediates. The major metabolites of sunset yellow are sulfanilic acid and amino-2-naphthol-6-sulfonic acid. Dye degradation products identified using LC-MS were sulfanilic acid with molecular mass 173.19 which appears as dimer with m/z value 340.4 and amino-2-naphthol-6-sulfonic acid with molecular weight 239.25, which also appears as dimer with m/z value 701.6 (Fig. 15). This confirmed that the degradation of sunset yellow took place efficiently in presence of cobalt doped titania.

Conclusion

An aqueous sol-gel method was used for the preparation of cobalt doped nano-TiO_2. The prepared materials were

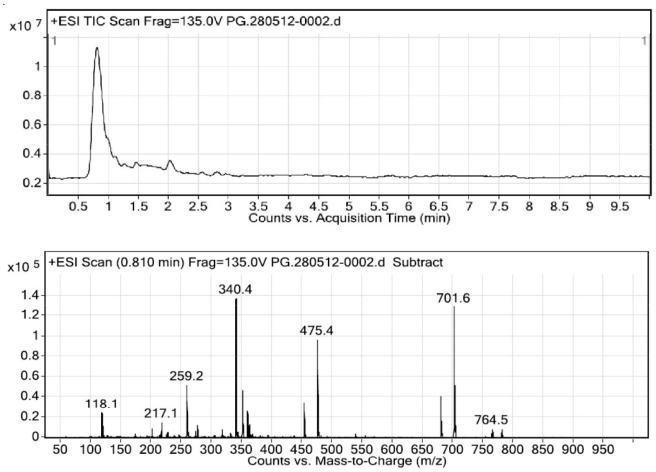

Fig. 15. LCMS of the degradation products of sunset yellow

analyzed using various physico-chemical characterization techniques. XRD analyses revealed the presence of mixed anatase and brookite phase of titania without any evidence for the rutile phase. Doping of cobalt in nano-TiO_2 lead to a decrease in particle size, an increase in surface area and low band gap value. The average particle size of the prepared samples ranged from 8-14 nm. TEM analyses revealed the spherical morphology of the particles without any aggregation of metal species. The calcined cobalt doped titania was found to be room temperature ferromagnetic while the as synthesized cobalt doped titania was diamagnetic. The photoactivity of the undoped and doped titania obtained by the degradation experiments of sunset yellow solution established that as synthesized cobalt doped TiO_2 was the better catalyst. The activity was found to be superior to that of commercial TiO_2 sample. The activity was depended on both the structural and textural characteristics of titania, evolved as a result of doping.

REFERENCES

1. Y. Matsumoto, M. Murakkami and T. Shono, *Science*, **291**, 854 (2001).
2. S.A. Chambers, S. Thevuthasan, R.F.C. Farrow, R.F. Marks, J.U. Thiele, L. Folks, M.G. Samant, A.J. Kellock, N. Ruzycki, D.L. Ederer and U. Diebold, *Appl. Phys. Lett*., **79**, 3476 (2001).
3. Y. Matsumoto, R. Takahashi, M. Murakami, T. Koida, X.J. Fan, T. Hasegawa, T. Fukumara, M. Kawasaki, S.Y. Koshihara and H. Koinuma, *J. Appl. Phys. (Japan)*, **40**, 1204 (2001).
4. J.J. Li, J.B. Zhu, L.T. Zhang, Y. Liu and W.C. Hao, *Asian J. Chem.*, **25**, 6173 (2013).
5. D.H. Kim, J.S. Yang, K.W. Lee, S.D. Bu, T.W. Noh, S.J. Oh, Y.W. Kim, J.S. Chung, H. Tanaka, H.Y. Lee and T. Kawai, *Appl. Phys. Lett*., **81**, 2421 (2002).
6. A. Manivannan, G. Glaspell and M.S. Seehra, *J. Appl. Phys*., **94**, 6994 (2003).
7. A. Manivannan, M.S. Seehra, S.B. Majumdar and R.S. Katiyar, *Appl. Phys. Lett*., **83**, 111 (2003).
8. Y.G. Joh, H.D. Kim, B.Y. Kim, S.I. Woo, S.H. Moon, J.H. Cho, E.C. Kim, D.H. Kim and C.R. Cho, *J. Korean Phys. Soc*., **44**, 360 (2004).
9. N.H. Hong, W. Prellier, J. Sakai and A. Ruyter, *J. Phys. Condens. Mater*., **16**, 5549 (2004).
10. J. Li, O.H. Sow, S.X. Rao, C.K. Ong and D.N. Zheng, *Eur. Phys. J. B*, **32**, 471 (2003).
11. K.A. Griffin, A.B. Pakhomov, C.M. Wang, S.M. Heald and K.M. Krishnan, *J. Appl. Phys*., **97**, 10D320 (2005).
12. T. Fukumara, H. Toyosaki, K. Ueno, M. Nakano and M. Kawasaki, *New J. Phys*., **10**, 055018 (2008).
13. G.M.H. van De Velde, S. Harkema and P.J. Gellings, *Inorg. Chem. Acta*, **11**, 243 (1974).
14. G. Jacobs, P.M. Patterson, Y. Zhang, T. Das, J. Li and B.H. Davis, *Appl. Catal. A*, **233**, 215 (2002).
15. M.K. Ahmad and M. Rusop, AIP Conf. Proc. 1136, 333; doi:http://dx.doi.org/10.1063/1.3160159.
16. R.I. Bickley and J.A. Navio, In eds.: G. Grassi and D.O. Hall, Photocatalytic Production of Energy-Rich Compounds, Elsevier, London, p. 297 (1985).
17. P. Kubelka and F. Munk, *Z. Technol. Phys*., **12**, 593 (1931).
18. C. Berlini, G. Ferraris, M. Guidotti, G. Moretti, R. Psaro and N. Ravasio, *Micropor. Mesopor. Mater*., **595**, 44 (2001).
19. C. Berlini, M. Guidotti, G. Moretti, R. Psaro and N. Ravasio, *Catal. Today*, **60**, 219 (2000).
20. L. Marchese, T. Maschmeyer, E. Gianotti, S. Coluccia and J.M. Thomas, *J. Phys. Chem. B*, **101**, 8836 (1997).
21. L. Marchese, E. Gianotti, T. Maschmeyer, G. Martra, S. Coluccia and J.M. Thomas, *Nuovo Cimento*, **19D**, 11 (1997).
22. L. Marchese, E. Gianotti, V. Dellarocca, T. Maschmeyer, F. Rey, S. Coluccia and J.M. Thomas, *Phys. Chem. Chem. Phys*., **1**, 585 (1999).
23. R. Hutter, T. Mallat and A. Baiker, *J. Catal*., **153**, 177 (1995).
24. A. Nilchi, S. Janitabar-Darzi and S. Rasouli-Garmarodi, *Mater. Sci. Appl*., **2**, 476 (2011).
25. N. Rajic, I. Arcon, V. Kaucic and A. Kodre, *Croatica Chem. Acta*, **72**, 645 (1999).
26. N. Venkatathri, *Bull. Catal. Soc. Ind*., **3**, 99 (2004).
27. X. Yan, J. He, D.G. Evans, X. Duan and Y. Zhu, *Appl. Catal. B*, **55**, 243 (2005).
28. S.K. Das, M.K. Bhunia and A. Bhaumik, *J. Solid State Chem*., **183**, 1326 (2010).
29. Z. Zhai, Y. Miao, Q. Sun, H. Tao, W. Wang and J. Wang, *Catal. Lett*., **131**, 538 (2009).
30. A. Doménech, A. Corma, H. García and S. Valencia, *Topics Catal*., **11**, 401 (2000).
31. A.K. Paul, M.A Prabu, G. Madras and S. Natarajan, *Chem. Sci*., **122**, 771 (2010).
32. S. AbouEl-Enein, F.A. El-Saied, S.M. Emam and M.A. Ell-Salamony, *Spectrochim. Acta A*, **71**, 421 (2008).
33. A.B.P. Lever, Inorganic Electronic Spectroscopy, Elsevier, Amsterdam, edn. 2 (1984).
34. D. Sutton, Electronic Spectra of Transition Metal Complexes, An Introductory Text, McGraw-Hill, London (1968).
35. J.D. Bryan, S.M. Heald, S.A. Chambers and D.R. Gamelin, *J. Am. Chem. Soc*., **126**, 11640 (2004).
36. J.M.D. Coey, A.P. Douvalis, C.B. Fitzerald and M. Venkatesan, *Appl. Phys. Lett*., **84** 1332 (2004).
37. J.M. Cho, W.J. Yun, J.K. Lee, H.S. Lee, W.W. So, S.J. Moon, Y. Jia, H. Kulkarni and Y. Wu, *Appl. Phys. A: Mater. Sci. Process*, **88**, 751 (2007).
38. T. Ohsaka, F. Izumi and J. Fujiki, *J. Raman. Spectrosc*., **7**, 321 (1978).
39. J. Yin, Z. Zou and J. Ye, *J. Phys. Chem. B*, **107**, 4936 (2003).
40. W. Zhu, X. Qiu, V. Lancu, X.Q. Chen, H. Pan, W. Wang, N.M. Dimitrijevic, T. Rajh, H.M. Meyer, M. Paranthaman, G.M. Stocks, H.H. Weitering, B. Gu, G. Eres and Z. Zhang, *Phys. Rev. Lett*., **103**, 226401 (2009).